Multiply Colored Electrochromic Carbazole-Based Polymers

Gregory A. Sotzing,† Jerry L. Reddinger,† Alan R. Katritzky,‡ Jadwiga Soloducho,‡ Richard Musgrave,‡ and John R. Reynolds*,†

Center for Macromolecular Science and Engineering and Center for Heterocyclic Compounds, Department of Chemistry, University of Florida, Gainesville, Florida 32611

Peter J. Steel

Department of Chemistry, University of Canterbury, Christchurch, New Zealand

Received December 10, 1996[⊗]

We report the synthesis and electrochemical polymerization of a series of bisheterocycle-*N*-substituted carbazoles. These monomers exhibit low peak oxidation potentials ($E_{p,m}$) which range from 0.15 to 0.46 V vs Ag/Ag^+, indicating facile polymerization. Repeated scan electrochemical polymerization for these monomers proceeds rapidly, relative to carbazole, to form stable electroactive films. Cyclic voltammetry of the polymers indicates that the films are well adhered to the electrode surface and that each of the polymers possess two distinct redox waves. At applied potentials greater than 1.15 V, a third irreversible oxidative process is observed, presumedly due to cross-linking. Optoelectrochemical analysis indicates that these polymers have an electronic bandgap (measured as the onset of the π-to-π^* transition) between 2.4 and 2.5 eV. Three distinct colors are achievable by varying the redox state of the polymers suggesting potential use for multiply colored electrochromic displays. For the series of bis(ethylenedioxythiophene)-*N*-substituted carbazoles, the fully reduced form of the polymers are canary yellow. Upon mild oxidation, the films become green and in the fully oxidized form, blue.

Introduction

The electrochemical polymerization of heterocyclic monomers to yield electronically conducting and redox electroactive polymers is well documented. Electrically conducting polymers have been considered for numerous applications including charge dissipation coatings,[1] organic thin-film transistors,[2] and conducting textiles.[3] The use of electrically conducting polymers in electrochromic devices, as materials that possess the ability to reversibly change color by altering redox state, has emerged.[4−9] Many conjugated polymers are colored in the neutral state since the energy difference between the π-bonding orbitals (conduction band) and the π^* antibonding orbitals (valence band) lies within the visible region. Upon oxidation, the intensity of the π-to-π^* transition decreases, and two low-energy transitions emerge to produce a second color. For example poly(3-methylthiophene) is red in the neutral state and blue in the oxidized state. While most electroactive polymers have the ability to exhibit two colors, only a select few show multiple color states.

Due to its accessibility and ease of handling, polyaniline (PANI) has become the conducting polymer of choice for many technological applications and has been studied extensively for its potential use as an electrochromic material. PANI is able to exist in three distinct reversible colored states; specifically yellow in the neutral state, green at 0.5 V vs SCE, and dark blue at 0.8V.[10−15] With multiple cycles, PANI tends to lose its ability to access these multicolor states. It has been shown, after 300 cycles between −0.2 and 1.0 V vs SCE, that the electrochromic activity of the film decreases as the color converts to semitransparent black with little change in color with variance in potential.[10,11]

An alternative to PANI for a multiply colored electrochromic polymer is polycarbazole. Previous work has shown poly(*N*-substituted carbazoles) to be clear colorless when neutral, green at an applied potential of 0.7 V vs SCE, and blue at 1.0 V.[16−18] The first report of

* To whom correspondence should be addressed.
† Center for Macromolecular Science and Engineering.
‡ Center for Heterocyclic Compounds.
⊗ Abstract published in *Advance ACS Abstracts,* May 1, 1997.

(1) Heywang, G.; Jonas, F. *Adv. Mater.* **1992**, *4*, 116
(2) Dodabalapur, A.; Torsi, L.; Katz, H. E. *Science* **1995**, *268*, 270.
(3) Kuhn, H. H.; Child, A. D.; Kimbrell, W. C. *Synth. Met.* **1995**, *71*, 2139.
(4) Druy, M. A.; Seymour, R. J. *J. Phys.* **1983**, *C3*, 595.
(5) Haynes, D. M.; Hepburn, A. R.; Goldie, D. M.; Marshall, J. M.; Pelter, A. *Synth. Met.* **1993**, *55−57*, 839.
(6) Panero, S.; Passerini, S.; Scrosati, B. *Mol. Cryst. Liq. Cryst.* **1993**, *229*, 97.
(7) Gustafsson, J. C.; Inganas, O.; Andersson, A. M. *Synth. Met.* **1994**, *62*, 17.
(8) Hyodo, K. *Electrochim. Acta* **1994**, *39*, 265.
(9) Nawa, K.; Imae, I.; Noma, N.; Shirota, Y. *Macromolecules* **1995**, *28*, 8, 723.
(10) Kobayashi, T.; Yoneyama, H.; Tamura, H. *J. Electroanal. Chem.* **1984**, *177*, 293.
(11) Kobayashi, T.; Yoneyama, H.; Tamura, H. *J. Electroanal. Chem.* **1984**, *161*, 419.
(12) Glarum, S. H.; Marshall, J. H. *J. Electrochem. Soc.* **1987**, *134*, 2160.
(13) Stilwell, D. E.; Park, S.-M. *J. Electrochem. Soc.* **1988**, *135*, 2497.
(14) Stilwell, D. E.; Park, S.-M. *J. Electrochem. Soc.* **1989**, *136*, 427.
(15) Chinn, D.; DuBow, J.; Liess, M. *Chem. Mater.* **1995**, *7*, 1504.
(16) Faid, K.; Ades, D.; Siove, A.; Chevrot, C. *J. Chim. Phys.* **1992**, *89*, 1019.
(17) Faid, K.; Siove, A.; Ades, D.; Chevrot, C. *Synth. Met.* **1993**, *55−57*, 1656.
(18) Faid, K.; Ades, D.; Siove, A.; Chevrot, C. *Synth. Met.* **1994**, *63*, 89.

S0897-4756(96)00630-8 CCC: $14.00 © 1997 American Chemical Society

the electrochemical polymerization of carbazole, carried out by Ambrose and Nelson, showed the most reactive sites for coupling to be the 3, 6, and 9 positions.[19] They also noted that coupling could proceed through the 1 and 8 positions; however, these positions are sterically hindered due to the rigid structure of carbazole. Dubois et al. further proposed that electrochemical oxidative polymerization occurred through the 3 and 6 positions.[20] The electrochemical polymerization of carbazole has also been studied in aqueous media under acidic conditions.[21,22] In one of our groups, we have previously prepared self-doped carbazole polymers which show two distinct redox processes.[23] Moreover, the electrochemical coupling of carbazole as a pendant to polymer supports has been studied.[24−27]

The disadvantages of directly polymerizing carbazole is that it requires a high potential for oxidation, and the polymerization proceeds rather sluggishly. Previously, other researchers[28−37] and ourselves[38−43] have presented the advantages of, and prepared multi-ring electropolymerizble monomers with electron-rich heterocycles at the terminal polymerization sites. By extending the conjugation of the monomer, large decreases are observed in the oxidation potential at which polymerization occurs, and the electroactive polymers exhibit a wide range of properties. To lower the oxidation potential of the monomer and control the optical and electronic properties of the polycarbazole, we have utilized pyrrole and 3,4-ethylenedioxythiophene (EDOT) in both the 3 and 6 positions of various N-substituted carbazoles.

Scheme 1

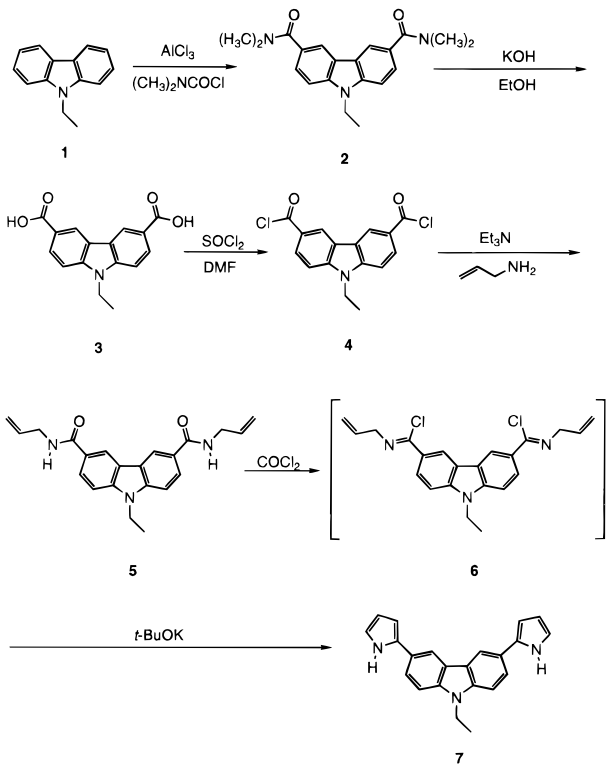

Here we detail the synthesis of five new highly conjugated carbazole-containing monomers that undergo polymerization at low oxidation potentials. These are 3,6-bis(pyrrol-2-yl)-9-ethylcarbazole (**7**, BP−NECz), 3,6-bis(2-(3,4-ethylenedioxy)thienyl)-*N*-methylcarbazole (**9a**, BEDOT−NMCz), 3,6-bis(2-(3,4-ethylenedioxy)-thienyl)-*N*-eicosylcarbazole (**9b**, BEDOT−NC20Cz), 3,6-bis(2-(3,4-ethylenedioxy)thienyl)-*N*-ethoxyethoxyethylcarbazole (**9c**, BEDOT−NGCz), and 3,6-bis(2-(3,4-ethylenedioxy)thienyl)-*N*-(4-(2-thienyl)butyl)carbazole (**9d**, BEDOT−NBTCz). The monomers were characterized by elemental analysis, FAB-HRMS, single-crystal X-ray structure determination (for **9a**), and ^{1}H and ^{13}C NMR and were electrochemically polymerized. The polymers were electrochemically characterized using cyclic voltammetry, and optoelectrochemistry. Previously, we have communicated the synthesis and electrochemical polymerization of both **9a** and **9c**[44] and examined the stability of poly(BEDOT−NMCz) in dual-polymer electrochromic devices.[45]

Results and Discussion

Synthesis of Bisheterocycle-*N*-substituted Carbazoles. The synthesis of 3,6-bis(pyrrol-2-yl)-9-ethylcarbazole (**7**, BP−NECz) is depicted in Scheme 1. This procedure is similar to the method we reported previously for the synthesis of aryl bispyrroles.[46] The first step involves the Lewis acid-catalyzed amidation of *N*-ethylcarbazole to give 9-ethylcarbazole-3,6-bis(dimethylcarbamide), **2**. Next the diamide was saponified to the diacid, **3**, followed by conversion to the diacid

(19) Ambrose, J. G.; Nelson, R. F. *J. Electrochem. Soc.* **1968**, *115*, 1159.
(20) Desbene-Monvernay, A.; Lacaze, P.-C.; Dubois, J.-E. *J. Electroanal. Chem.* **1981**, *129*, 229.
(21) Cattarin, S.; Mengoli, G.; Musiani, M. M.; Schreck, B. *J. Electroanal. Chem.* **1988**, *246*, 87.
(22) Mengoli, G.; Musiani, M. M.; Schreck, B.; Zecchin, S. *J. Electroanal. Chem.* **1988**, *246*, 73.
(23) Qiu, Y.-J.; Reynolds, J. R. *J. Electrochem. Soc.* **1990**, *137*, 900.
(24) Grazulevicius, J. V.; Kublickas, R. *Eur. Polym. J.* **1991**, *27*, 1411.
(25) Hepburn, A. R.; Marshall, J. M.; Maud, J. M. *Synth. Met.* **1991**, *41−43*, 2935.
(26) Geibler, U.; Hallensleben, M. L. *Synth. Met.* **1993**, *55−57*, 1662.
(27) Mazeika, R.; Grazulevicius, J. V.; Kavaliunas, R.; Kreiveniene, N. *Eur. Polym. J.* **1994**, *30*, 319.
(28) Danieli, R.; Ostoja, R.; Tiecco, M.; Zamboni, R.; Taliani, C. *J. Chem. Soc., Chem Commun.* **1986**, 1473.
(29) Ferraris, J. P.; Skiles, G. D. *Polymer* **1987**, *28*, 179.
(30) Tanaka, S.; Kaeriyama, K.; Hiraide, T. *Makromol. Chem., Rapid Commun.* **1988**, *9*, 743.
(31) Kaeriyama, K.; Tanaka, S. *Makromol. Chem.* **1988**, *189*, 1755.
(32) Ferraris, J. P.; Andrus, R. G.; Hrncir, D. C. *J. Chem. Soc., Chem. Commun.* **1989**, 1318.
(33) Pelter, A.; Maud, J. M.; Jenkins, I.; Sadeka, C.; Coles, G. *Tetrahedron Lett.* **1989**, *30*, 3461.
(34) Roncali, J.; Gorgues, A.; Jubault, M. *Chem. Mater.* **1993**, *5*, 1456.
(35) Haynes, P. M.; Hepburn, A. R.; Goldie, D. M.; Marshall, J. M.; Pelter, A. *Synth. Met.* **1993**, *55−57*, 839.
(36) Lorcy, D.; Cava, M. P. *Adv. Mater.* **1992**, *4*, 562.
(37) Kitamura, C.; Tanaka, S.; Yamashita, Y. *J. Chem. Soc., Chem. Commun.* **1994**, 1585.
(38) Sotzing, G. A.; Reynolds, J. R.; Steel, P. J. *Chem. Mater.* **1996**, *8*, 882−889.
(39) Child, A. D.; Sankaran, B.; Larmat, F.; Reynolds, J. R. *Macromolecules* **1995**, *28*, 6571.
(40) Reynolds, J. R.; Katritzky, A. R.; Soloducho, J.; Belyakov, S.; Sotzing, G.; Pyo, M. *Macromolecules* **1994**, *27*, 7225.
(41) Reynolds, J. R.; Child, A. D.; Ruiz, J. P.; Hong, S. Y.; Marynick, D. S. *Macromolecules* **1993**, *26*, 2095.
(42) Ruiz, J. P.; Dharia, J. R.; Reynolds, J. R.; Buckley, L. J. *Macromolecules* **1992**, *25*, 849.
(43) Reynolds, J. R.; Ruiz, J. P.; Child, A. D.; Nayak, K.; Marynick, D. S. *Macromolecules* **1991**, *24*, 678.
(44) Reddinger, J. L.; Sotzing, G. A.; Reynolds, J. R. *J. Chem. Soc., Chem. Commun.* **1996**, 1777.
(45) Sapp, S. A.; Sotzing, G. A.; Reddinger, J. L.; Reynolds, J. R. *Adv. Mater.* **1996**, *8*, 808.
(46) Sotzing, G. A.; Reynolds, J. R.; Katritzky, A. R.; Soloducho, J.; Belyakov, S.; Musgrave, R. *Macromolecules* **1996**, *29*, 1679.

Scheme 2

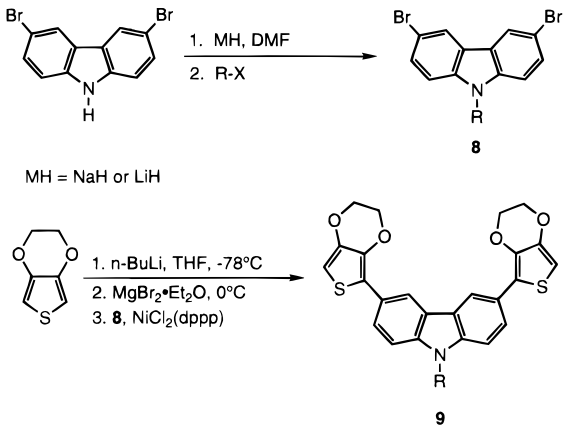

8 **9**

R		X	Yield		Yield
-CH_3	**8a**	I	72%	**9a**	62%
-$(CH_2)_{19}CH_3$	**8b**	Br	65%	**9b**	73%
-$(CH_2CH_2O)_2CH_2CH_3$	**8c**	OTs	68%	**9c**	68%
-$(CH_2)_4$-thienyl	**8d**	Br	50%	**9d**	72%

chloride, **4**, utilizing $SOCl_2$. Compound **4** was then reacted with allyl amine in the presence of triethylamine to give the bis(allylamide), **5**. Subsequent treatment of **5** with phosgene gave the carbazole bis(allylimino chloride), **6**, which was used without isolation or purification in the following step. Ring closure of the bis(allylimino chloride) was effected under basic conditions to give BP−NECz in an overall synthetic yield of 5.8%.

The synthesis of the BEDOT−*N*R−Cz's (**9a**−**d**) is depicted in Scheme 2. The preparation of 3,6-dibromo-*N*-substituted carbazoles was carried out utilizing either sodium hydride or lithium hydride for hydrogen abstraction in anhydrous DMF, followed by addition of the appropiate alkylating agent (either methyl iodide, eicosyl bromide, bromobutylthiophene, or 2-(ethoxy(ethoxy))-ethyl tosylate). Addition of the terminal EDOT moieties was effected utilizing a $NiCl_2$(dppp) catalyzed cross-coupling of the aforementioned dibromo-*N*-substituted carbazole with the Grignard reagent of EDOT. Overall yields from 3,6-dibromocarbazole ranged from ca. 25 to 50%.

Structural Analysis. The structure of BEDOT-NMCz was determined by single-crystal X-ray crystallography at −105 °C. Figure 1 shows a perspective view and atom labeling of the contents of the asymmetric unit, which comprises a full molecule of BEDOT−NMCz and a molecule of chloroform solvate, which is disordered over two orientations. Tables 1 and 2 list the atomic coordinates and the bonding geometry, respectively.

The potential symmetry of the BEDOT−NMCz molecule in the crystal is destroyed by torsional differences. Although both of the inter-ring bonds are in s-trans orientations, there is a significant difference in the degree of twisting about these bonds. Whereas one thiophene ring (S1′−C5′) is approximately coplanar with the plane of the carbazole system (angle between mean planes = 8.2(3)°), the other (S1″−C5″) is significantly twisted out of the plane of the carbazole (angle between meanplanes = 26.2(3)°). This twisting does not seem to be due to the presence of the chloroform solvate molecule; indeed the shortest intermolecular contact is between a chloroform chlorine atom and the sulfur atom (S1′) of the thiophene ring, which is coplanar with the carbazole. It should be noted in Figure 1 that the shortest intermolecular distance between the chloroform and the BEDOT−NMCz is not shown. The molecules

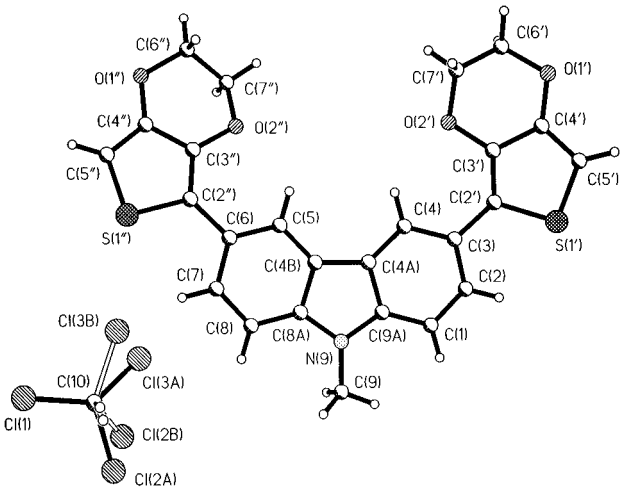

Figure 1. Single-crystal X-ray structure and atom labeling for BEDOT−NMCz.

Table 1. Atomic Coordinates (×10⁴) and Equivalent Isotropic Displacement Coefficients (Å² × 10³)

atom	*x*	*y*	*z*	U_{eq}[a]
C1	15228(2)	2633(5)	106(2)	38(1)
C2	15078(2)	1796(5)	−405(2)	38(1)
C3	14127(2)	1487(5)	−702(2)	32(1)
C4	13286(2)	2054(4)	−451(1)	29(1)
C4A	13420(2)	2906(4)	64(1)	27(1)
C4B	12747(2)	3682(5)	425(1)	27(1)
C5	11702(2)	3788(5)	389(1)	27(1)
C6	11268(2)	4641(5)	817(1)	30(1)
C7	11897(3)	5447(5)	1262(2)	36(1)
C8	12915(3)	5353(5)	1302(2)	37(1)
C8A	13343(2)	4438(5)	889(2)	30(1)
N9	14339(2)	4117(4)	839(1)	34(1)
C9A	14395(2)	3206(5)	344(2)	32(1)
C9	15182(3)	4572(5)	1248(2)	47(1)
S1′	15072(1)	227(2)	−1597(1)	50(1)
C2′	14016(2)	664(5)	−1260(2)	34(1)
C3′	13189(3)	167(5)	−1614(1)	33(1)
C4′	13399(3)	−582(5)	−2137(2)	39(1)
C5′	14385(3)	−606(6)	−2181(2)	50(1)
O1′	12669(2)	−1184(4)	−2540(1)	48(1)
C6′	11733(3)	−1291(8)	−2325(2)	88(2)
C7′	11501(3)	−111(8)	−1931(2)	87(2)
O2′	12225(2)	343(3)	−1480(1)	40(1)
S1″	9622(1)	6140(1)	1233(1)	42(1)
C2″	10180(2)	4658(5)	829(1)	29(1)
C3″	9482(2)	3532(5)	605(1)	28(1)
C4″	8504(2)	3861(5)	764(2)	34(1)
C5″	8471(3)	5200(5)	1107(2)	39(1)
O1″	7699(2)	2866(3)	580(1)	44(1)
C6″	7886(2)	1804(5)	111(2)	42(1)
C7″	8891(2)	971(5)	230(2)	38(1)
O2″	9677(2)	2194(3)	269(1)	34(1)
C10	11792(4)	11485(6)	1772(2)	63(1)
C11	10904(1)	12328(2)	2185(1)	65(1)
C12A[b]	13038(7)	11666(16)	2248(2)	85(2)
C12B[c]	12725(5)	10575(17)	2187(2)	100(3)
C13A[b]	11772(17)	9599(8)	1492(3)	157(6)
C13B[c]	11089(4)	9847(6)	1348(2)	76(2)

[a] Equivalent isotropic *U* defined as one-third of the trace of the orthogonalized U_{ij} tensor. [b] Disordered; occupancy 44%. [c] Disordered; occupancy 56%.

Table 2. Bond Lengths (Å) and Angles (deg)

C1−C2	1.365(5)	C1−C9A	1.389(5)	C2−C3	1.408(5)
C3−C4	1.410(4)	C3−C2′	1.457(5)	C4−C4A	1.378(5)
C4A−C9A	1.419(4)	C4A−C4B	1.449(5)	C4B−C5	1.404(4)
C4B−C8A	1.410(5)	C5−C6	1.396(4)	C6−C7	1.419(5)
C6−C2″	1.470(4)	C7−C8	1.367(5)	C8−C8A	1.390(5)
C8A−N9	1.385(4)	N9−C9A	1.378(4)	N9−C9	1.446(4)
S1′−C5′	1.697(4)	S1′−C2′	1.742(3)	C2′−C3′	1.367(5)
C3′−O2′	1.380(4)	C3′−C4′	1.424(5)	C4′−C5′	1.345(5)
C4′−O1′	1.368(4)	O1′−C6′	1.415(5)	C6′−C7′	1.378(6)
C7′−O2′	1.400(5)	S1″−C5″	1.715(4)	S1″−C2″	1.737(4)
C2″−C3″	1.358(5)	C3″−O2″	1.366(4)	C3″−C4″	1.434(4)
C4″−C5″	1.337(5)	C4″−O1″	1.371(4)	O1″−C6″	1.432(4)
C6″−C7″	1.505(5)	C7″−O2″	1.432(4)		

C2−C1−C9A	118.0(3)	C1−C2−C3	123.5(3)
C2−C3−C4	117.9(3)	C2−C3−C2′	121.0(3)
C4−C3−C2′	121.1(3)	C4A−C4−C	119.6(3)
C4−C4A−C9A	120.5(3)	C4−C4A−C4B	134.0(3)
C9A−C4A−C4B	105.5(3)	C5−C4B−C8A	119.9(3)
C5−C4B−C4A	133.0(3)	C8A−C4B−C4A	107.1(3)
C6−C5−C4B	119.2(3)	C5−C6−C7	119.0(3)
C5−C6−C2″	121.5(3)	C7−C6−C2″	119.5(3)
C8−C7−C6	122.3(3)	C7−C8−C8A	118.4(3)
N9−C8A−C8	129.9(3)	N9−C8A−C4B	109.0(3)
C8−C8A−C4B	121.1(3)	C9A−N9−C8A	108.5(3)
C9A−N9−C9	125.1(3)	C8A−N9−C9	126.3(3)
N9−C9A−C1	129.6(3)	N9−C9A−C4A	109.8(3)
C1−C9A−C4A	120.5(3)	C5′−S1′−C2′	92.7(2)
C3′−C2′−C3	131.7(3)	C3′−C2′−S1′	108.6(3)
C3−C2′−S1′	119.7(3)	C2′−C3′−O2′	123.8(3)
C2′−C3′−C4′	114.5(3)	O2′−C3′−C4′	121.7(3)
C5′−C4′−O1′	125.5(3)	C5′−C4′−C3′	111.7(4)
O1′−C4′−C3′	122.8(3)	C4′−C5′−S1′	112.5(3)
C4′−O1′−C6′	112.0(3)	C7′−C6′−O1′	118.8(4)
C6′−C7′−O2′	119.3(4)	C3′−O2′−C7′	113.3(3)
C5″−S1″−C2″	93.0(2)	C3″−C2″−C6	129.4(3)
C3″−C2″−S1″	109.3(2)	C6−C2″−S1″	120.9(3)
C2″−C3″−O2″	124.2(3)	C2″−C3″−C4″	113.4(3)
O2″−C3″−C4″	122.4(3)	C5″−C4″−O1″	124.4(3)
C5″−C4″−C3″	113.4(3)	O1″−C4″−C3″	122.1(3)
C4″−C5″−S1″	110.9(3)	C4″−O1″−C6″	112.1(3)
O1″−C6″−C7″	110.6(3)	O2″−C7″−C6″	111.0(3)
C3″−O2″−C7″	111.8(2)		

pack in the typical herringbone pattern often found for aromatic compounds.

The repeat unit structure of the polymer may be indirectly related with the structure of the monomer in the solid state. It should be noted that crystal packing forces can provide significant effects in determining inter-ring torsional angles. In the structure of BEDOT−NMCz, one of the EDOT rings is able to attain a nearly planar conformation relative to the carbazole. As the polymer prepared by electropolymerization/deposition is disordered and amorphous, we expect a significant portion of the chain to be nearly planar. Therefore, the possibility of a significant amount of interchain transport is possible.

Oxidative Polymerization. All monomers were electrochemically polymerized using repeated potential scan polymerization with a standard three-electrode cell. Scheme 3 illustrates the oxidative electrochemical polymerization for the BEDOT−*N*R−Cz's. The oxidative polymerization is believed to proceed through the α positions of the external heterocyclic rings since the 3, 6, and 9 positions of the carbazole are blocked. The external rings contain a higher electron density and the oxidations occur at quite low potentials.

Figure 2 depicts the repeated potential scan electropolymerization of BEDOT−NGCz in 0.1 M tetrabutylammonium perchlorate/acetonitrile (TBAP/ACN) and is representative for all of the monomers. Initially, the potential is set at a nonoxidative potential, −0.8 V, and is scanned anodically at a scan rate of 100 mV/s. At 0.33 V there is an onset for the monomer oxidation ($E_{onset,m}$) with a peak at 0.42 V ($E_{p,m}$), at which polymerization occurs. Upon reductive scanning, a cathodic process is observed corresponding to the reduction of as-deposited oxidized polymer. During the second anodic scan, an oxidation attributed to the polymer is

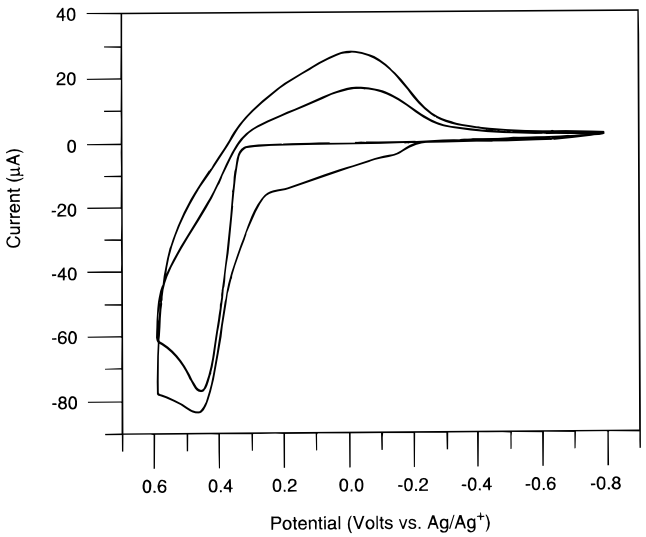

Figure 2. Repeated potential scanning polymerization of 0.01 M BEDOT−NGCz in 0.1 M TBAP/ACN at a scan rate of 100 mV/s.

Scheme 3

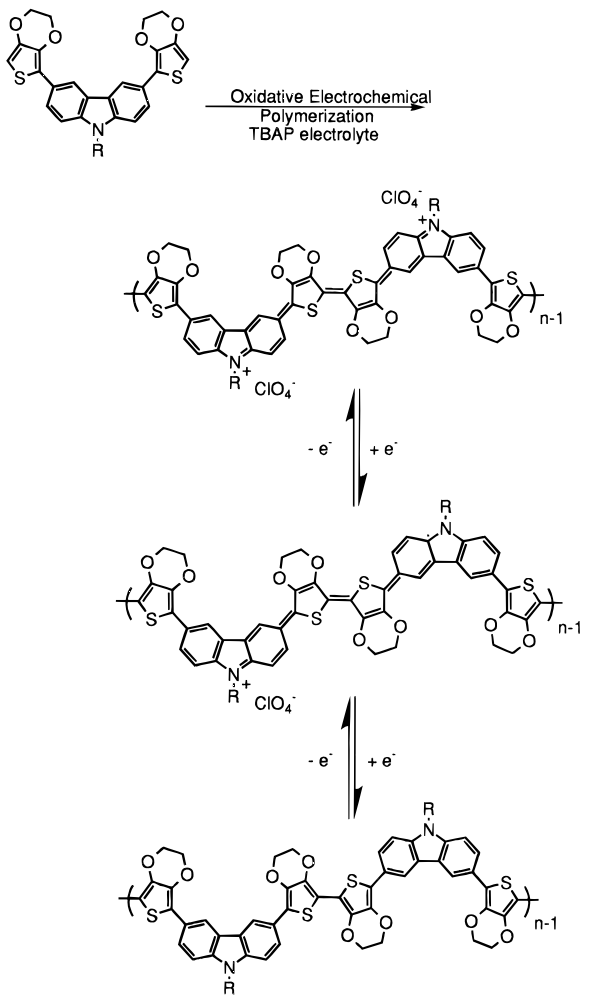

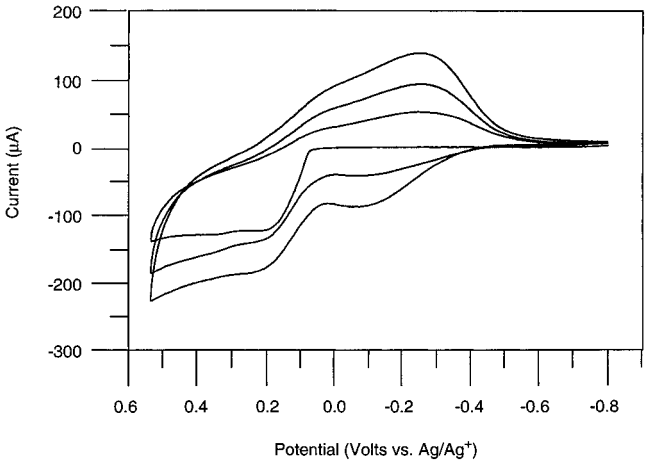

Figure 3. Repeated potential scanning polymerization of 0.01 M BP−NEC in 0.1 M TBAP/ACN at a scan rate of 100 mV/s.

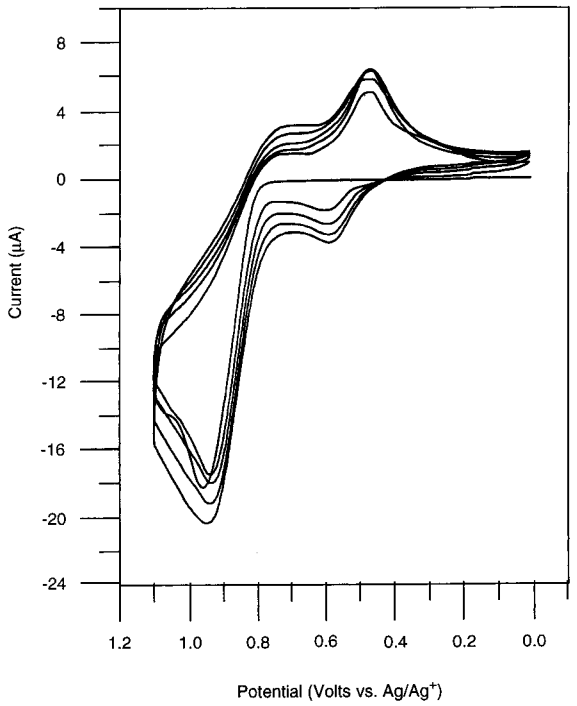

Figure 4. Repeated potential scanning polymerization of 0.01 M carbazole in 0.1 M TBAP/ACN at a scan rate of 100 mV/s.

observed with an onset at ca. −0.2 V followed by further monomer oxidation and polymerization. Upon repeated scanning, the current response of both the anodic and cathodic polymer redox processes increase, the result of the deposition of electroactive conducting polymer.

Figure 3 shows the repeated potential scan polymerization for BP−NEC. The polymerization begins at an $E_{onset,m}$ of 0.09 V with an $E_{p,m}$ at 0.15 V. This $E_{p,m}$ is ca. 0.30 V lower than that for the BEDOT−*N*R−Cz's which can be attributed to the external pyrroles being more electron rich than the external EDOT's. Both of these bisheterocycle carbazoles electropolymerize at much lower potentials and quite rapidly relative to the single-ring heterocyclic monomers, pyrrole, EDOT, and carbazole. For comparison purposes, the repeated potential scanning polymerization of carbazole is illustrated in Figure 4. This monomer exhibits an $E_{p,m}$ at 0.93 V, 0.5−0.8 V higher than the EDOT and pyrrole analogues, respectively. As shown from the slow increase of the polymer redox current response with

Table 3. Electrochemical Properties for Carbazole-Based Monomers and Their Polymers

monomer	$E_{onset,m}$[a]	$E_{p,m}$[a]	$E_{1/2,p1}$[a]	$E_{1/2,p2}$[a]	E_g[b]
BP−NEC[c]	0.09	0.15	0.02	0.53	2.5
BEDOT−NMC[c]	0.28	0.36	0.19	0.46	2.4
BEDOT−NC20Cz[d]	0.34	0.46	0.23	0.55	2.4
BEDOT−NGCz[c]	0.33	0.42	0.21	0.50	2.4
BEDOT−NBTCz[c]	0.34	0.43	0.21	0.50	2.4
carbazole	0.88	0.95	0.65	0.91	N/A

[a] Values listed as volts vs Ag/Ag^+ reference electrode. [b] Values listed in electronvolts as the onset of the $\pi-\pi^*$ transition. [c] Performed in 0.1 M TBAP/ACN, 10 mM monomer. [d] Performed in 0.1 M TBAP/50:50 CH_2Cl_2/ACN, 10 mM monomer.

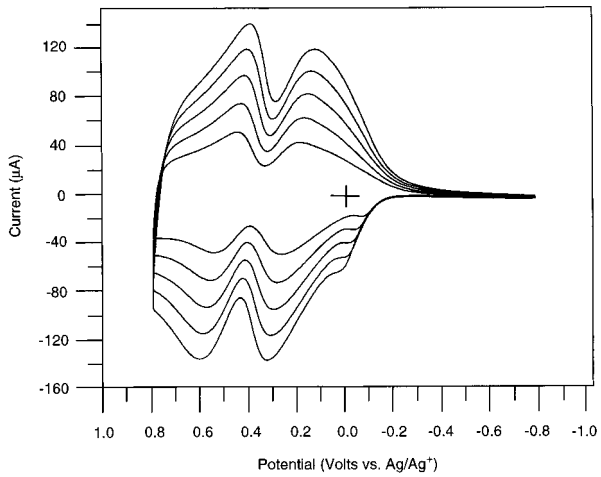

Figure 5. Cyclic voltammetry of poly(BEDOT−NGCz) in 0.1 M TBAP/ACN at scan rates of 100, 200, 300, 400, and 500 mV/s.

multiple scans, polymerization proceeds much more sluggishly than that for the bisheterocycle carbazoles. Table 3 gives a compilation of the $E_{onset,m}$ and $E_{p,m}$ values for all systems studied. BP−NEC (containing unsubstituted external pyrrole rings) exhibits an $E_{p,m}$ that is 0.26 V lower than 3,6-bis(*N*-methylpyrrol-2-yl)-*N*-ethylcarbazole, previously prepared and reported by Geibler et al.[47] This can be explained by steric hindrance induced between the pyrrole and carbazole moieties by the methyl groups.

N-substitution (ranging from methyl to eicosyl) of carbazole within the bis(EDOT) series was found to have little effect on the oxidation potential of the monomer. This is expected since the N-alkylation site is removed from the external rings. As such, there is no torsional distortion imposed on the rings within the monomers or significant electronic effects to cause a change in oxidation potentials. We find this to be the case for all four bis(EDOT) monomers and expect that there will not be steric interactions with any group substituted on the carbazole nitrogen.

Polymer Electrochemistry. Cyclic voltammetry was used to probe the accessible redox states in all of the carabazole-based polymers as deposited by the repeated scanning method. This is illustrated as a function of scan rate for poly(BEDOT−NGCz) in Figure 5. It should be noted that all of the carbazole based polymers exhibited two separate redox processes under 1 V. The observation of the two dominant redox processes, and thus the presence of three separate charge states, is typical of polymers containing the

(47) Geibler, U.; Hallensleben, M. L. *Synth. Met.* **1993**, *55−57*, 1483.

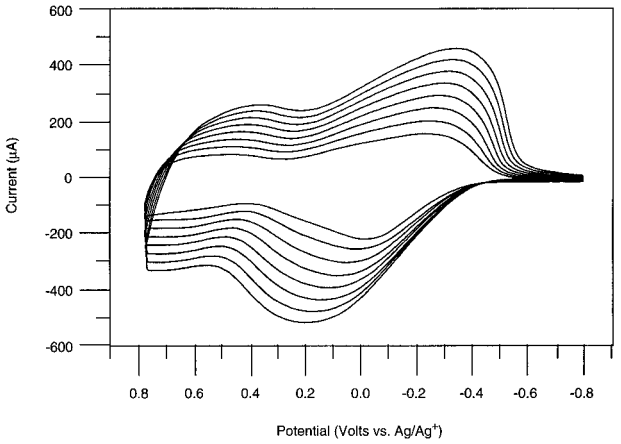

Figure 6. Cyclic voltammetry of poly(BP−NEC) in 0.1 M TBAP/ACN at scan rates of 150, 200, 250, 300, 350, 400, 450, and 500 mV/s.

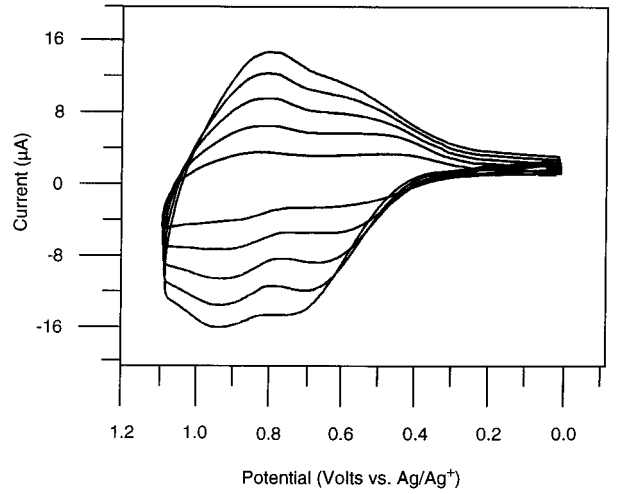

Figure 7. Cyclic voltammetry of poly(carbazole) in 0.1 M TBAP/ACN at scan rates of 100, 200, 300, 400, and 500 mV/s.

bicarbazole moiety. The biheterocycle linkage between carbazoles along the chain yields a discrete electroactive site of increased conjugation length as illustrated by the cation-radical and dication states in Scheme 3. In contrast to polypyrroles and polythiophenes, carbazole-linked polymers are not fully conjugated. Instead, their conjugation is broken at the carbazole nitrogen atom causing the cation-radical and dication charge carriers to be localized between bicarbazole units. This illustrates the importance of interchain transport processes in these polymers.

To confirm that the electroactive site is electrode surface confined, the peak current for the polymer redox was probed as a function of scan rate during cyclic voltammetry. In each case, the current was found to scale linearly with the scan rate for each polymer, indicating that the migration of the electroactive species is not diffusion controlled; hence, the polymer films are electrode supported. Figure 6 shows the scan rate dependency for poly(BP−NEC). The first of the two redox processes of this polymer is centered around 0 V with a broad peak-to-peak separation. The second redox process occurs at a higher potential of 0.53 V. For comparison purposes, the scan rate dependency for the redox cycling of polycarbazole is shown in Figure 7. Both of these polymers exhibit redox processes that are less distinct than that found for the full series of BEDOT−*N*R−Cz's. In addition, polycarbazole oxidizes at a much higher potential than that found for both of the poly(bisheterocycle carbazoles) illustrating the importance of the extended conjugation within the electroactive center. Table 3 lists the potentials for both the first half wave redox process ($E_{1/2,p1}$) and the second half wave redox process ($E_{1/2,p2}$) for each polymer. Again the most easily oxidized of the series is poly(BP−NEC) due to the increased electron richness of the polymer.

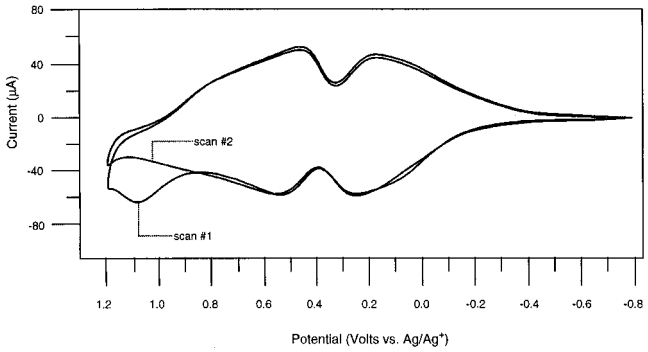

Figure 8. Cyclic voltammetry of poly(BEDOT-NMCz) in 0.1 M TBAP/ACN at a scan rate of 100 mV/s.

In the course of examining these polymers redox properties for electrochromic applications, a higher potential irreversible oxidation was discovered. Figure 8 shows the cyclic voltammetry (first two scans) for a poly(BEDOT−NMCz) film, prepared by repeated scanning between −0.8 to 0.7 V and subsequently cycled at a scan rate of 100 mV/s from −0.8 to 1.2 V in monomer-free electrolyte. After equilibration of the polymer redox by repeated scanning between −0.8 and 0.8 V, a third redox process is observed with a peak potential of 1.1 V. This process disappears upon the second excursion to high potential. It should be noted that the first two redox processes show essentially no change in current response, indicating that the electroactive portion of the polymer is not undergoing any chemical or electrochemical degradation. Repeated potential excursions to 1.2 V yield a current response identical with scan 2 for up to 10 scans. This phenomenon was found to be general for these BEDOT polymers as it has been observed for poly(BEDOT−NMCZ), poly(BEDOT−NGCZ), and poly(BEDOT−NC20CZ). Both poly(BP−NEC) and poly(BEDOT−NBTCZ) were stable only up to 1.1 V, thereby rendering the observation of the third oxidative process impossible.

Faid et al. prepared phenylene−carbazolylene copolymers in which the third oxidative process in the polymer cyclic voltammetry was suggested to be the oxidation of biphenylene subunits within the polymer backbone.[16−18] By analogy, this would suggest that the third oxidative process observed in our polymers would be due to the bis(EDOT) linkages. If this were the case, the third oxidative process should be coupled to a reversible reduction and be reproducible upon subsequent electrochemical cycling. However, for our systems the third oxidation is seen only on the first excursion of the polymer to high potential and is irreversible. This indicates that an electrochemical oxidation is followed by an irreversible chemical reaction. We propose that cross-linking of the polymer through open sites on the carbazole moiety within the polymer is occurring.

Further evidence supporting this cross-linking reaction comes from the observation of the third oxidative

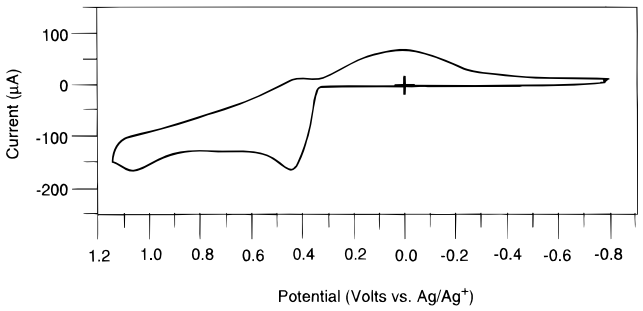

Figure 9. Cyclic voltammetric polymerization (−0.8 to 1.2 V) of BEDOT−NMCz (0.01 M) in 0.1 M TBAP/ACN at a scan rate of 100 mV/s.

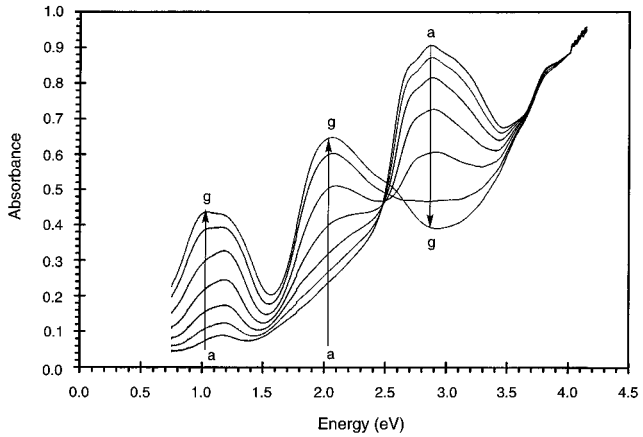

Figure 10. Optoelectrochemical analysis performed on poly(BEDOT−NC20Cz) in 0.1 M TBAP/ACN with (a) −1.2, (b) −0.2, (c) −0.10, (d) 0, (e) 0.10, (f) 0.20, and (g) 0.30 V vs Ag/Ag^+.

process when the monomers were polymerized via potential scanning polymerization between −0.8 and 1.15 V as shown for BEDOT−NMCz in Figure 9. Upon washing and equilibrating the polymer-modified electrode with electrolyte, a cyclic voltammogram between −0.8 and 1.15 V indicates no evidence of a third oxidative process (only the two reversible redox processes of the polymer were present). Another process known to occur at high potentials is oxidative degradation of the polymer, often termed overoxidation. Since the current response remains unchanged after the third oxidative process, the possibility of overoxidation can be disregarded since this process would lead to a loss in the polymer electroactivity. To structurally prove that cross-linking occurred, an attempt at obtaining the IR spectrum of the polymer obtained from constant-potential electrochemical polymerization at 0.7 and 1.2 V was attempted; however, the aromatic C−H stretching vibrations were weak and undiscernible.

Electronic Structure. Optoelectrochemical analysis of the above polymers was performed in order to elucidate electronic transitions present upon doping and undoping of the polymer. Figure 10 shows a series of optoelectrochemical spectra performed for poly(BEDOT−NC20Cz) and is representative for all the poly(BEDOT-*N*-substituted carbazoles). Full reduction of the polymer was achieved by electrochemically reducing at an applied potential of −1.2 V. As indicated by the spectrum obtained at −1.2 V, the polymer is slightly doped; therefore, in some instances we utilized an additional hydrazine reduction to compensate small amounts of trapped charge in the films and observe a reduction in the intensity of these low-energy absorbances.[44] In the reduced form, there is an onset for the absorption of the polymerat 2.4 eV, representing the π-to-π^* transition which is denoted as the bandgap (E_g) for convential conducting polymers such as polypyrrole and polythiophene. However, for these carbazole-based systems, the conjugation of the conducting polymer is broken at the nitrogens of the carbazole moiety, thus leading to discrete cationic units located throughout the polymer backbone. Little is known about the mode of conductivity in polycarbazole and the optoelectronic transistions that exist upon doping. Since the systems presented here exhibit optoelectrochemical behavior similar to conventional conducting polymers, the data will be presented as such. The polymers' λ_{max} is observed at 2.9 eV. All of the BEDOT-*N*-substituted polymers were found to exhibit the E_g's of 2.4 eV with λ_{max} at 2.9 eV, with the exception of poly(BEDOT−NGCz) which was found to exhibit an E_g of 2.5 eV with λ_{max} occurring at 2.8 eV.

After the initial full reduction, the polymer was electrochemically oxidized at −0.2 V. At this potential, the onset of the first oxidation of the polymer is evident in the cyclic voltammogram (Figure 5). Upon sequential oxidation, it is evident in Figure 10 that the intensity of the higher energy interband transition decreases, while two lower energy transitions evolve. The lower energy transition process (E_{b1}) occurs with a λ_{max} at 1.1 eV, while the higher energy transition (E_{b2}) is observed at a λ_{max} of 2.1 eV. Progressively oxidizing the polymer up to an applied potential of 0.3 V causes the two lower energy transitions to become well-defined and more intense, while the higher energy absorption continues to decrease in intensity. By removing electrons from the conduction band via electrochemical oxidation, the polymer is converted from the aromatic "flexible" structure to the oxidized quinoidal form (Scheme 3). Such a geometrical change results in charge carriers which create two states within the gap. The lower energy transition (E_{b1}) for all of the poly(BEDOT-*N*-substituted carbazoles) is observed at a λ_{max} of 1.1 eV while the higher energy transition (E_{b2}) is observed at 2.1 eV. Figure 10 is representative of fully conjugated polythiophenes in that E_{b1} and E_{b2} increase in intensity while the interband transition decreases in intensity upon continual oxidation of the polymer.

Figure 11 shows the optoelectrochemical analysis of poly(BEDOT−NC20Cz) at higher applied potentials. The initial oxidative applied potential is 0.4 V, and upon oxidation to 0.5 V, E_{b1} continues to increase in intensity and shifts to a higher energy, while E_{b2} decreases in intensity and shows a slight increase in the energy of the absorption. When the applied potential is increased to a maximum of 0.8 V, E_{b1} reaches a maximum intensity. At the same time, E_{b2} continues to decrease in intensity.

Unlike the series of poly(BEDOT)-*N*-substituted carbazoles, poly(BP−NEC) was unstable at high potentials and exhibited quite different optoelectrochemical behavior. It should be noted that in order to fully reduce the electrochemically prepared poly(BP−NEC), it was necessary to utilize hydrazine reduction, followed by rinsing the polymer film with acetonitrile. As shown in Figure 12, the UV−vis−NIR spectrum of the reduced

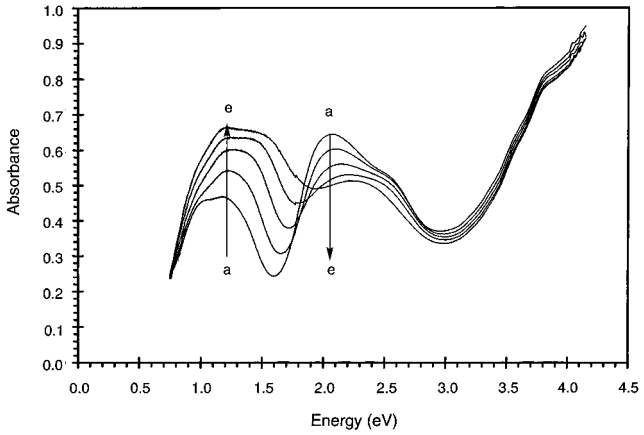

Figure 11. Optoelectrochemical analysis performed on poly(BEDOT−NC20Cz) in 0.1 M TBAP/ACN at applied potentials of (a) 0.40, (b) 0.50, (c) 0.60, (d) 0.70, and (e) 0.80 V vs Ag/Ag^+.

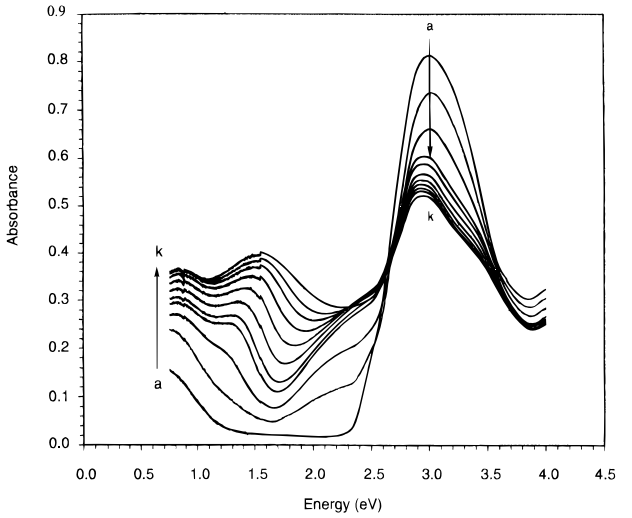

Figure 12. Optoelectrochemical analysis performed on poly(BP−NEC) in 0.1 M TBAP/ACN at applied voltages of (a) −0.9, (b) −0.2, (c) −0.1, (d) 0.0, (e) 0.1, (f) 0.2, (g) 0.3, (h) 0.4, (i) 0.5, (j) 0.6, and (k) 0.8 V vs Ag/Ag^+.

polymer shows two absorbances. The typical high-energy absorption is indicative of the interband transition, with an E_g of 2.5 eV and a λ_{max} of 3.0 eV. The lower energy transition, λ_{max} of <0.8 eV is not yet understood; however, it could indicate that the polymer is not fully reduced. This is not surprising due to the facile oxidation of the poly(BP−NEC) (see Table 3). Upon initial oxidation of the polymer, this lower energy transition increases in intensity and is accompanied by the emergence of two other low-energy transitions. While this phenomenon is consistent with the transformation to the doped states, full explanation of the spectral changes is difficult. Further studies utilizing in situ electron paramagnetic resonance (EPR) and conductivity measurements during electrochemical doping are being used to study this.

Electrochromic Properties. The electrochromic properties of the poly(BEDOT−*N*-substituted carbazoles) differ significantly from those found in polythiophenes and polypyrroles. While these systems possess only two accessible colored states, all of the poly(BEDOT-*N*-substituted carbazole) films achieve three distinct colored states. These polymers are transmissive canary yellow when fully reduced, transmissive lime green upon oxidation up to the tail of the first oxidative process, and dark blue upon full oxidation. While similar behavior is exhibited by polyaniline (PANI) the redox switching stability of the PBEDOT−N−Cz's has allowed us to use them in high-contrast electrochromic polymer devices with long switching lifetimes.[45] Furthermore, the fact that these carbazole monomers can be N-substituted with flexible substituents allows soluble and processable electrochromic materials to be prepared.

Conclusion

We have prepared a series of carbazole monomers containing extended conjugation in good yields which undergo facile electrochemical polymerization to yield stable, electroactive conducting polymers. Incorporating carbazole into the main chain of the polymer limits the length of conjugation in the neutral polymer and thereby gives rise to a high bandgap material. The polymer cyclic voltammetry indicates that the polymer may exist in three distinct redox states. While poly(BP−NEC) exhibits electrochromic properties similar to PPy, the series of poly(BEDOT-*N*-substituted carbazoles) were found to exhibit multiple colored states (yellow−green−blue) corresponding to the different redox states which are similar to those associated with PANI. The poly(BEDOT−*N*-substituted carbazole) systems were found to be highly stable to electrochemical cycling, deemed useful for industrial applications.

Experimental Section

Reagents. EDOT was obtained from AG Bayer and was vacuum distilled before use. 3,6-Dibromocarbazole, anhydrous DMF, sodium hydride, lithium hydride, magnesium bromide etherate ($MgBr_2 \cdot 2Et_2O$), [bis(diphenylphosphino)propane]-nickel(II) chloride, and 9-ethylcarbazole were used as received from Aldrich. Carbazole was recrystallized from ethanol. *n*-BuLi was used as received from ACROS. TBAP was purchased from Sigma and was recrystallized from ethanol and dried under vacuum before use. THF was distilled over potassium/benzophenone ketyl under nitrogen prior to use, and acetonitrile was distilled over calcium hydride. Column chromatography was performed using Merck Keiselgel 60 (5386) silica gel. All reactions were carried out under an inert atmosphere of either prepurified nitrogen or argon.

Instrumentation. All NMR spectra were acquired at 300 MHz using either $CDCl_3$ or DMSO-d_6 as a solvent unless otherwise stated. All experiments involving the use of a potentiostat were performed on an EG&G Princeton Applied Research Model 273 potentiostat/galvanostat. Optoelectrochemical analysis was obtained using a Varian Cary 5E UV−vis-NIR spectrophotometer.

9-Ethylcarbazole-3,6-bisdimethylcarbamide (2). To a stirred mixture of aluminum chloride (1.33 g, 1 mmol) and ethylene chloride (10 mL) under nitogen was added a solution of **1** (1 g, 5 mmol) dissolved in ethylene chloride (10 mL). A solution of dimethylcarbamyl chloride (1.07 g, 10 mmol) in ethylene chloride (10 mL) was added dropwise over 10 min. The mixture was heated at reflux for 18 h under nitrogen, cooled, and treated with water (10 mL). The organic layer was washed with water, until the washings were neutral to litmus, and dried over magnesium sulfate. The solvent was evaporated under reduced pressure and the product washed with hexane to give **4a**. Yield 1.40 g (81%). Mp 217−218 °C [lit. 218−220 °C].[48]

9-Ethylcarbazole-3,6-dicarboxylic acid (3). A mixture of **2** (1.0 g, 2.9 mmol), and 20% ethanolic potassium hydroxide was heated under reflux for 6 h. The solvent was evaporated,

(48) Domanski, A.; Kyziol, J. B. *Pol. J. Chem.* **1985**, *59*, 613.

the residue taken up into water, and the solution acidified with concentrated hydrochloric acid. The precipitate was collected by filtration and washed with water. Recrystallization from benzene gave white needles of **3**. Yield 0.50 g (63%). Mp 315 °C [lit. >300 °C].[49]

9-Ethylcarbazole-3,6-dicarbonyl Chloride (4). A mixture of **3** (1.0 g, 3.5 mmol), thionyl chloride (12.68 mL, 175 mmol), and DMF (1 drop) under nitrogen was stirred for 12 h at room temperature. The solution was heated at 80 °C, and the excess thionyl chloride removed simultaneously by distillation. The residual solid was washed with chloroform to give **4**, which was used directly in the next step. Yield 0.73 g (64%). Mp 201 °C [lit. 203 °C].[50]

3,6-*N*,*N*-Diallylcarbamide-9-ethylcarbazole (5). A solution of **4** (1.0 g, 3.1 mmol) in dry benzene (30 mL) was added slowly with vigorous stirring to a solution of allylamine (0.37 g, 6.6 mmol) and triethylamine (0.6 g, 6 mmol) in dry benzene. The mixture was stirred at room temperature for 10 h, heated at reflux for 1 h, cooled, and poured into diethyl ether (50 mL). The precipitate was filtered and recrystallization from methanol gave colorless needles of **4**. Yield 0.65 g (57%). Mp 165 °C. ^{1}H NMR δ ($CDCl_3$) 1.34 (t, 3 H, *J* 7.0 Hz, NCH_2CH_3), 3.99 (t, 4 H, *J* 5.35 Hz, $NH-CH_2$), 4.51 (q, 2 H, *J* 7.0 Hz, NCH_2-CH_3), 5.12 (d, 2 H, *J* 10.2 Hz, CH=CHH cis), 5.23 (d, 2 H, *J* 17.2 Hz, C=CHH trans), 5.95 (m, 2 H, $CH=CH_2$), 7.72 (d, 2 H, *J* 8.8 Hz, H-1), 8.08 (d, 2 H, *J* 8.5 Hz, H-2), 8.70 (t, 2 H, *J* 5.6 Hz, NH), 8.82 (s, 2 H, H-4); ^{13}C NMR δ (DMDO-d_6) 13.7 (CH_3), 37.4 (NCH_2CH_3), 41.6 ($NH-CH_2$), 109.0 (C-1), 115.0 ($CH=CH_2$), 120.0 (C-2), 121.9 (C-3, C-4a), 125.6 (C-4), 135.7 ($CH=CH_2$), 141.7 (C-8a), 166.3 (CONH). Anal. Calcd for $C_{22}H_{23}N_3O_2$: C, 71.09; H, 6.71; N, 10.36. Found: C, 71.28; H, 6.76; N, 10.34.

3,6-Bis(pyrrol-2-yl)-9-ethylcarbazole (7). A mixture of **5** (1 g, 2.7 mmol), phosgene (20% solution in toluene, 21 mL), and DMF (1 drop) was stirred for 24 h at room temperature, and the solvent evaporated to dryness under reduced pressure. The resulting crude bischloroimine **6** was used without isolation or purification in the next step. A solution of crude **6** in THF (30 mL) was added dropwise with stirring to potassium *tert*-butoxide (1.12 g, 10 mmol) in a mixture of THF (30 mL) and DMF (6 mL) at 5−10 °C under nitrogen. After stirring for 30 min at this temperature, the reaction mixture was poured into ice water and extracted with chloroform (2 × 50 mL). The organic phase was dried ($MgSO_4$) and evaporated to dryness, and the residue subjected to column chromatography (hexane:ethyl acetate 1:3) to give **7**. Yield 0.25 g (31%). Mp 134 °C. ^{1}H NMR δ ($CDCl_3$) 1.45 (t, 3 H, 7.3 Hz, NCH_2CH_3), 4.33 (q, 2 H, 7.2 Hz, NCH_2CH_3), 6.35 (br s, 2 H, H-4′), 6.54 (br s, 2 H, H-3′), 6.89 (br s, 2 H, H-5′), 7.36 (d, 2 H, *J* 8.5 Hz, H-1), 7.61 (d, 2 H, *J* 8.5 Hz, H-2), 8.16 (s, 2H, H-4), 8.49 (br s, 2 H, NH); ^{13}C NMR δ (DMSO-d_6) 13.8 (NCH_2CH_3), 37.7 (NCH_2CH_3), 104.8 (C-1), 108.9 (C-4′), 109.9 (C-3′), 115.8 (C-5′), 118.1 (C-2), 122.9 (C-4), 123.2 (C-4a), 124.4 (C-2′), 133.3 (C-3), 139.1 (C-8a). HRMS Calcd for $C_{22}H_{19}N_3$: 325.1579 (M^+). Found: 325.1546.

3,6-Dibromo-*N*-methylcarbazole (8a). To a three-necked round-bottom flask equipped with nitrogen purge and reflux condenser was added 6.0 g (0.0185 mol) of 3,6-dibromocarbazole along with 75 mL of anhydrous DMF. To the stirred solution was added 0.72 g (0.030 mol) of sodium hydride. Immediately a yellow precipitate formed with evolution of hydrogen gas. This was stirred for a further 15 min to dissolve the carbazole anion; then 4.26 g (0.030 mol) of iodomethane was added in one portion. The reaction was exothermic, indicating the reaction proceeded immediately. After 5 h, 200 mL of water was added to give a light brown precipitate. After recrystallization from chloroform, 2.7 g (43%) of long light brown needles were obtained. Mp 118−121 °C; ^{1}H NMR δ ($CDCl_3$) 8.431 (d, 2 H, 1-H), 7.585 (m, 4 H, 2-H and 4-H), 3.842 (s, 3 H, $-CH_3$); ^{13}C NMR δ ($CDCl_3$) 29.255, 111.212 , 11.405, 122.735, 123.243, 128.731, 139.580. Anal. Calcd for $C_{13}H_9NBr_2$: C, 46.1; H, 2.68; N, 4.13. Found: C, 46.61; H, 2.68; N, 4.08. HRMS Calcd for $C_{13}H_9NBr_2$: 336.9102 (M^+). Found: 336.9099.

3,6-Dibromo-*N*-eicosylcarbazole (8b). 3,6-Dibromo-*N*-eicosanylcarbazole was prepared following the same procedure as that for 3,6-dibromo-*N*-methylcarbazole using the following: 9.2 g (28.3 mmol) of 3,6-dibromocarbazole, 2.0 g (83.3 mmol) of sodium hydride, and 10.5 g (29 mmol) of 1-bromoeicosane. The reaction was allowed to continue for 13 h, followed by precipitation from water. The crude product was reprecipitated from methylene chloride to give 11.05 g (64.5%) of white powder. Mp 82−85 °C; ^{1}H NMR δ ($CDCl_3$) 0.882 (m, 3 H, −CH3), 1.215 (m, 34 H, $-CH2-$), 1.784 (m, 2 H, −CH2-), 4.227 (m, 2 H, $N-CH2-$), 7.332 (d, 2 H, H-1), 7.521 (d, 2 H, H-2), 8.125 (s, 2 H, H-4); FAB-HRMS Calcd for $C_{32}H_{47}NBr_2$: 603.2075 (M^+). Found: 603.2081.

3,6-Dibromo-*N*-[(ethoxyethoxy)ethyl]carbazole (8c). To a solution of 6.5 g (20 mmol) of 3,6-dibromocarbazole dissolved in 50 mL of anhydrous DMF was added 0.176 g (20 mmol) of lithium hydride. This was allowed to stir for 15 min after which 6.07 g (20 mmol) of the tosylate of (ethoxyethoxy)ethanol was added in one portion. The reaction was allowed to continue for 5 h. The solution was then poured into water and filtered, and the precipitate recrystallized from ethanol/hexane (2:1) to give 6.02 g (68.2%) of white solid. ^{1}H NMR δ (DMSO-d_6) 1.131 (t, 3H), 3.410 (m, 6H), 3.811 (t, 2H), 4.392 (t, 2H), 7.302 (d, 2H), 7.527 (d, 2H), 8.076 (s, 2H); ^{13}C NMR δ (DMSO-d_6)15.042, 43.517, 66.638, 69.282, 69.769, 70.991, 110.710, 112.125, 123.014, 123.462, 128.936, 139.505. Anal. Calcd for $C_{18}H_{19}NO_2Br_2$: C, 49.01; H, 4.34; N, 3.17; Br, 36.22. Found: C, 48.91; H, 3.87; N, 2.99; Br, 35.89.

3,6-Dibromo-*N*-(4-(2-thienyl)butyl)carbazole (8d). To a solution of 2.99 g (9.2 mmol) of 3,6-dibromocarbazole dissolved in 50 mL of anhydrous DMF was added 0.11 g (9.2 mmol) of lithium hydride in one portion. This was allowed to stir for 15 min. Then, 3.02 g (9.2 mmol) of 4-bromo-1-(2-thienyl)butane was added, and the reaction allowed to continue for 6 h. The solution was poured onto ice to yield a brownish solid. The solid was then recrystallized from methanol/$CHCl_3$ (50:50) to give 2.13 g (50.0%) of 3,6-dibromo-*N*-(4-(2-thienyl)-butyl)carbazole. ^{1}H NMR δ ($CDCl_3$) 1.722 (m, 2H), 1.851 (m, 2H), 2.812 (t, 2H), 4.211 (t, 2H), 6.697 (d, 1H), 6.708 (t, 1H), 7.085 (d, 1H), 7.106 (d, 2H), 7.503 (d, 2H), 8.100 (s, 2H); ^{13}C NMR δ ($CDCl_3$) 27.756, 28.624, 28.704, 42.151, 111.232, 111.552, 122.882, 123.376, 12.351, 124.351, 126.741, 128.737, 138.986, 144.327. Anal. Calcd for $C_{20}H_{17}NSBr_2$: C, 51.86; H, 3.70; N, 3.02; S, 6.92; Br, 34.50. Found: C, 51.84; H, 3.58; N, 2.93; S, 7.21; Br, 34.13.

3,6-Bis(2-(3,4-ethylenedioxy)thienyl)-*N*-methylcarbazole (9a). To a three-necked round-bottom flask equipped with nitrogen purge was added 200 mL of THF and 1.68 g (11.8 mmol) of ethylenedioxythiophene. The solution was cooled to −78 °C via a dry ice/acetone bath. After temperature equilibration, 5.0 mL of 2.5 M (12.5 mmol) *n*-BuLi in hexanes was added via syringe. After stirring for 30 min, 3.2 g (12.4 mmol) of magnesium bromide etherate was added in one portion and allowed to stir for another thirty minutes. Then 2.0 g (5.90 mmol) of 8a was added along with 0.6 g (9.3 mol %) of $NiCl_2$·dppp. The reaction was allowed to continue for 20 h. The solution was poured onto ice to yield brown precipitate. This was washed with pentane to give 3.4 g (62.5%) of white solid. Mp 219−220 °C; ^{1}H NMR δ (DMSO-d_6) 3.879 (s, 3 H, $-CH_3$), 4.278, 4.368 (s, 4H, $-OCH_2CH_2O-$), 6.562 (s, 2 H, 2′-H), 7.613 (d, 2 H, H-1), 7.790 (d, 2 H, H-2), 8.382 (s, 2 H, H-4). Anal. Calcd for $C_{25}H_{19}O_4NS_2$: C, 63.02; H, 4.15; N, 3.03; S, 13.91. Found: C, 62.39; H, 3.99; N, 2.66; S, 14.26. HRMS Calcd for $C_{25}H_{19}O_4NS_2$: 461.0756 (M^+). Found: 461.0749.

3,6-Bis(2-(3,4-ethylenedioxy)thienyl)-*N*-eicosylcarbazole (9b). BEDOT−NC_{20}Cz was prepared in a similar procedure as BEDOT−NMCz using the following: 5.70 g (33.1 mmol) of 3,4-ethylenedioxythiophene, 13.6 mL of 2.5 M (34.0 mmol) *n*-BuLi in hexanes, 8.78 g (34.0 mmol) magnesium bromide etherate, 10.0 g (16.6 mmol) of **8b** and 0.3 g (10 mol %) of $NiCl_2$·dppp. The reaction was allowed to continue for 18 h after the addition of $NiCl_2$·dppp. Precipitation from water

(49) Albrecht, W. L.; Fleming, R. W.; Horgan, S. W.; Mayer, G. D. *J. Med. Chem.* **1977**, *20*, 364.

(50) Negodyaev, N. D.; Pushkareva, Z. V. *Khim. Geterotsikl. Soedin.* **1966**, 586; *Chem. Abstr.* **1967**, *66*, 28605n.

and reprecipitation from methylene chloride yielded 8.89 g (73.8%) of a white solid. Mp 86−88 °C; ^{1}H NMR δ (DMSO-d_6) 0.821 (t, 3H), 1.127 (m, 36H), 1.746 (m, 2H), 4.273 (m, 4H), 4.353 (m, 4H), 6.544 (s, 2H), 7.573 (d, 2H), 7.736 (d, 2H), 8.353 (s, 2H). Anal. Calcd for $C_{44}H_{57}O_4NS_2$: C, 73.18; H, 7.14; N, 1.94; S, 8.87. Found: C, 72.38; H, 7.98; N, 1.83; S, 8.04. HRMS Calcd for $C_{44}H_{57}O_4NS_2$: 727.3729 (M^+). Found: 727.3701.

3,6-Bis(2-(3,4-ethylenedioxy)thienyl)-*N*-[(ethoxyethoxy)-ethyl]carbazole (9c). BEDOT−NGCz was prepared in a manner similar to BEDOT−NMCz using 1.54 g (10.8 mmol) of EDOT, 4.4 mL of 2.5 M *n*-BuLi in hexanes, 50 mL of THF, 2.84 g (11.0 mmol) of $MgBr_2 \cdot Et_2O$, 2.2 g (10.8 mmol) of **8c**, and 0.050 g (0.09 mmol, 1 mol %) of $NiCl_2$(dppp). After 18 h of reaction time, the reaction mixture was poured into water, the precipitate was filtered and recrystallized from chloroform to give 1.922 g (68.4%) of BEDOT−NGCz as a white solid. Mp 122−124 °C; ^{1}H NMR δ ($CDCl_3$) 1.140 (t, 3H), 3.426 (m, 6H), 3.842 (t, 2H), 4.270 (s, 4H), 4.328 (s, 4H), 4.459 (t, 2H), 6.277 (s, 2H), 7.427 (d, 2H), 7.794 (d, 2H), 8.396 (s, 2H); ^{13}C NMR δ ($CDCl_3$) 15.056, 43.257, 64.735, 66.611, 69.222, 70.984, 96.228, 96.315, 109.040, 118.287, 118.327, 118.635, 123.188, 124.490, 124.757, 136.962, 139.866, 142.236. Anal. Calcd for $C_{30}H_{29}NO_6S_2$: C, 63.92; H, 5.19; N, 2.48; S, 11.38. Found: C, 63.25; H, 4.97; N, 2.37; S, 11.69. HRMS Calcd for $C_{30}H_{29}NO_6S_2$: 564.1515 (M^+). Found: 564.1565.

3,6-Bis(2-(3,4-ethylenedioxy)thienyl)-*N*-(4-(2-thienyl)-butyl)carbazole (9d). BEDOT−NBTCz was prepared in a manner similar to BEDOT−NMCz except using the following amounts of reagents: 0.77 g (5.4 mmol) of EDOT, 2.2 mL of 2.5 M *n*-BuLi in hexanes, 50 mL of THF, 1.39 g (5.4 mmol) of $MgBr_2 \cdot Et_2O$, 1.19 g (2.7 mmol) of 3,6-dibromo-*N*-(4-(2-thienyl)-butyl)carbazole, and 50 mg (0.09 mmol, 3.3 mol %) of $NiCl_2$-(dppp). The reaction mixture was poured into water, and the solid filtered and recrystallized from ethanol/hexane (2:1) to give 1.13 g (71.7%) of white product. ^{1}H NMR δ ($CDCl_3$) 1.745 (m, 2H), 1.913 (m, 2H), 2.833 (t, 2H), 4.294 (m, 6H), 4.366 (m, 4H), 6.296 (s, 2H), 6.724 (d, 1H), 6.899 (t, 1H), 7.101 (d, 1H), 7.262 (d, 2H), 7.819 (d, 2H), 8.426 (s, 2H); ^{13}C NMR δ (DMSO-d_6) 28.288, 29.243, 29.490, 42.836, 64.528, 64.742, 96.255, 108.773, 118.434, 118.461, 118.628, 123.028, 123.114, 124.290, 124.764, 126.706, 136.928, 139.612, 142.209, 144.453. Anal. Calcd for $C_{32}H_{27}NO_4S_3$ C: 65.62; H, 4.65; N, 2.39; S, 16.42. Found: C, 65.22; H, 4.37; N, 2.24; S, 15.91. HRMS Calcd for $C_{32}H_{27}NO_4S_3$: 586.1181 (M^+). Found: 586.1116.

X-ray Crystallography: Data Collection, Structure Solution, and Refinement. Intensity data were collected with a Nicolet P4s four-circle diffractometer using monochromatized Mo Kα (λ = 0.710 73 Å) radiation. The crystal used was a colorless block of dimensions 0.86 × 0.21 × 0.17 mm. Throughout data collection the intensities of three standard reflections were monitored at regular intervals and the intensities were corrected for minor decay (<3%). The intensities were also corrected for Lorentz and polarization effects but not for absorption.

The structure was solved by direct methods using SHELXS90[51] and refined on F^2 by full-matrix least-squares procedures using SHELXL96.[52] All non-hydrogen atoms were refined with anisotropic displacement coefficients. Hydrogen atoms were included in calculated positions with isotropic displacement coefficients equal to 1.2 times the isotropic equivalent of their carrier carbons. The function minimized was $\sum w(F_o^2 - F_c^2)$, with $w = [\sigma^2(F_o^2) + 0.051P^2]^{-1}$, where $P = [\max(F_o^2) + 2F_c^2]/3$. A final difference map showed no features greater or less than 0.39 e^{-3}/Å. Final non-hydrogen atom coordinates, bond lengths, and bond angles are listed in Tables 1 and 2.

Crystal data at −105 °C: $C_{26}H_{20}Cl_3NO_4S_2$, Mr = 580.9, monoclinic, space group $P2_1/n$, a = 13.482(1), b = 7.931(2), c = 23.484(1) Å, β = 96.73(1)°, U = 2493.7(4) Å^3, $F(000)$ = 1192, Z = 4, D_c = 1.547 g cm^{-3}, μ(Mo Kα) = 5.71 cm^{-1}, ω scans, $2\theta_{max}$ = 50°, 345 parameters, $wR2$ = 0.106 for all 4380 data, $R1$ = 0.048 for 2238 data with $F_o > 4\sigma(F_o)$.

Acknowledgment. We would like to thank both the Air Force Office of Scientific Research (F49620-96-1-0067) and the National Science Foundation (CHE-9629854) for financial support of this work.

CM960630T

(51) Sheldrick, G. M. *Acta Crystallogr., Sect. A.* **1990**, *46*, 467.
(52) Sheldrick, G. M., SHELXL-96, University of Gottingen, 1996.